Journal of Crystal Growth 108 (1991) 114–120
North-Holland

Triggering explosive crystallization of amorphous silicon

A. Polman *, S. Roorda, P.A. Stolk and W.C. Sinke

FOM-Institute for Atomic and Molecular Physics, Kruislaan 407, 1098 SJ Amsterdam, The Netherlands

Received 30 March 1990; manuscript received in final form 22 August 1990

The initial stages of explosive crystallization (EC) of amorphous Si (a-Si) are investigated. A thin layer of liquid Si (l-Si), highly undercooled with respect to crystalline Si (c-Si) is formed by nanosecond pulsed ruby laser irradiation of a-Si prepared by ion implantation. Time-resolved reflectivity measurements are used to determine the time delay in the onset of EC for different surface structures. If a thin single crystal layer of Si covers the a-Si, EC proceeds immediately. In the absence of a seed for EC, a maximum time delay of 11 ± 2 ns is observed. Intermediate delay times are found if the surface layer contains small c-Si clusters.

1. Introduction

Explosive crystallization of amorphous silicon is an interesting phenomenon, which is often observed during nanosecond pulsed-laser irradiation of the material [1–8]. Basically, explosive crystallization (EC) involves the following phase transformation sequence. An amorphous Si (a-Si) layer on top of a crystalline (c-Si) substrate (usually produced by ion implantation) is irradiated with a low-energy (≈ 0.1 J/cm^2) nanosecond laser pulse. During irradiation, a shallow region of a-Si at the surface is heated and melted. The temperature of this "primary" liquid (l-Si) layer is then near the melting point of a-Si, which is estimated to be ≈ 225 K below that of c-Si ($T_{ma} \approx 1460$ K [1], $T_{mc} = 1685$ K). Hence, highly undercooled l-Si is formed, which will tend to crystallize. If the a-Si surface layer is covered by a thin layer of single crystal Si (in which case the a-Si is actually a buried layer), a crystal seed is present and the undercooled melt solidifies to epitaxial c-Si [9,10]. In the absence of this seed, c-Si grains have to nucleate, after which growth of these grains at the expense of the undercooled melt occurs. The amorphous → liquid → crystal transition is exothermic due to the difference in latent heat of melting for c-Si and a-Si [11] and part of the released heat can be used for deeper melting, resulting in formation of a "secondary" melt. Subsequent solidification of this secondary melt again gives a heat release, which induces further melting. In this way a continuous, self-sustained ("explosive") crystallization process, mediated by a moving buried liquid layer, converts the a-Si to c-Si. The typical velocities of the buried layer are in the range 8–15 m/s [4–7]. Transmission electron microscopy (TEM) has shown that epitaxial EC yields single crystal Si, epitaxially aligned with the c-Si top-layer [9,10] and that unseeded EC generally yields randomly oriented poly-Si with a typical grain size of ≈ 100 Å [1,3,7,8]. Lowndes et al. have shown that for a detailed description of all microstructural changes during EC, two-dimensional effects have to be taken into account. From a detailed microstructural analysis [7] and from model calculations [8] they have inferred that heat-flow and crystal growth in a lateral direction (i.e. perpendicular to the surface normal) play an important role during the initiation of EC.

At present, a fundamental question concerning EC has remained unanswered: "What is the nature of the nucleation processes that trigger and

* Present address: AT&T Bell Laboratories, Murray Hill, New Jersey 07947, USA.

sustain EC?". Two different nucleation scenarios have been suggested to describe unseeded EC of a-Si:

(1) Tsao and Peercy [12] have shown, on the basis of theoretical arguments, that a moving l-Si/a-Si interface can be unstable with respect to nucleation of c-Si. Under certain assumptions, this can explain both triggering and sustaining of EC: c-Si nuclei form at the melt-in interface and grow in the surrounding undercooled liquid, supplying heat for deeper melting.

(2) Roorda and Sinke [13] have suggested that solid-state nucleation in the heating phase prior to melting could play a role in both the triggering and sustaining of EC. They suggest that small crystallites can nucleate in a-Si during heating. Due to their higher melting temperature, these c-Si nuclei would remain solid during melting of the a-Si in which they are imbedded, whereupon they could rapidly grow in the surrounding undercooled liquid.

Bulk nucleation in undercooled l-Si, which has also been suggested as a mechanism to explain EC [5], can be excluded, especially in view of recent measurements by Stiffler et al. [14].

Nucleation usually is a two-step process as a function of time: first a transient time is necessary to build up a steady-state population of metastable nuclei, i.e. nuclei with a sub-critical size. This stage is followed by steady-state nucleation. In the Tsao/Peercy model the melt-in interface is moving at high speed and hence is refreshed continuously. This implies that this type of nucleation can only play a role if the transient time is negligible. At present it is not clear if this is realistic or not. In the Roorda/Sinke model a transient time also plays a role. However, this delay time becomes less important if one assumes that sub-critical nuclei which are formed in a-Si can be stabilized (as in the Tsao/Peercy model) at the l-Si/a-Si interface [13]. Sub-critical nuclei are present in large concentration and are formed in a time shorter than the transient time. Unfortunately little information is available on the transient time and nucleation rate in a-Si at high temperatures. It should be noted that nucleation in a-Si at high temperatures is indeed observed in experiments concerning lateral EC [15].

In this paper a comparison will be made between epitaxial and unseeded EC of a-Si, with special attention to the timing of the initial stages of EC. A range of samples was prepared, some containing a buried amorphous layer, separated from the surface by a crystalline layer and others with an a-Si surface layer. The thickness of the c-Si surface layer varied from one sample to the other in the range between 0 and 60 nm. Using pulsed-laser irradiation, EC was initiated in all samples. From a time-resolved study of the solidification phenomena it is possible to estimate the typical time scales involved in nucleation and growth.

2. Experimental

Ion implantation was used to form a-Si layers in a single-crystalline substrate. A 4 inch Si(100) wafer was implanted at room temperature with 450 keV $^{63}Cu^+$ ions to a total dose of 1.5×10^{15} cm^{-2}. The ion beam was scanned electrostatically over the wafer with a maximum scan angle amplitude of 1.5°. The target was tilted 7°, with the tilt axis parallel to a wafer flat. This yielded a planar channeling geometry in the middle of the wafer. However, due to the large angular deviation, the scanned ion beam became increasingly "random" towards the edge of the wafer. It is known that planar channeling conditions can lead to formation of a buried a-Si layer, whereas, for the same implantation dose, random conditions can result in formation of an a-Si layer at the surface. Using the above implantation scheme, a continuous range of structures was obtained on one wafer. One piece of the wafer was additionally implanted in a random direction with 80 keV $^{28}Si^+$ to a total dose of 5×10^{15} cm^{-2}. All implantations were performed at room temperature using an ion beam with a peak beam current density of ≈ 4 $\mu A/cm^2$.

Samples were irradiated with a single pulse from a Q-switched ruby laser (wavelength $\lambda = 694$ nm, pulse duration 32 ns full width at half maximum). Using a diaphragm and a lense, a small spatial fraction of the laser beam was projected on the sample under far-field conditions. During irradiation, the transient optical reflectivity [16] of

the sample was monitored using a continuous wave AlGaAs laser operating at $\lambda = 825$ nm. Calculations of the reflectivity of a l-Si layer underneath a c-Si layer of a certain thickness show that interference minima and maxima occur with a period of 100 nm, the first minimum occurring for a c-Si thickness of 40 nm. The time-resolved reflectivity (TRR) technique probes changes in refractive index and hence, in combination with proper modelling, makes it possible to follow phase transformations in real time.

Microstructural analyses were performed employing Rutherford backscattering spectrometry and channeling [17] using a 1.9 MeV He^+ beam and a scattering angle of 105°. In addition, Raman spectroscopy was performed using the $\lambda =$ 514.5 nm line from an Ar ion laser.

3. Surface structure

3.1. Channeling

Fig. 1 shows channeling spectra taken on various positions over the wafer, numbered 1 to 6. The spectrum for spot 1 shows a region with a reduced yield in the energy region below the Si surface backscattering energy. This indicates that a surface layer with crystalline order has remained after implantation. The thickness of this layer is estimated to be ≈ 60 nm. The spectrum for spot 2, which was implanted more "randomly", shows a thinner region (≈ 40 run) with crystalline ordering at the surface. For spots 3, 4 and 5, channeling does not indicate the presence of crystalline material at the surface. However, a very low density of micro-crystalline clusters in the amorphous matrix, which cannot be detected by channeling, is likely to remain at the surface under the present implantation conditions.

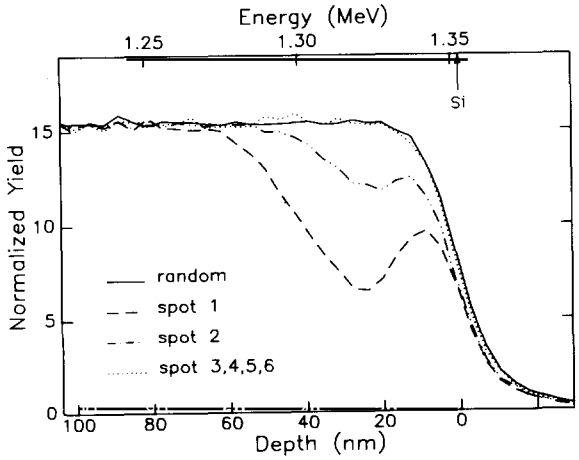

Fig. 1. Channeling spectra for Si (100) samples implanted with 450 keV Cu^+ ions to a dose of 1.5×10^{15} cm^{-2}. The implantation geometry ranged from planar channeling to random. A random spectrum is shown for reference. The arrow indicates the Si surface backscattering energy.

The effect of such clusters has previously been observed by Iverson and Reif [18], who studied solid phase nucleation (at 630°C) in ion implanted a-Si. They found three regimes of crystallization as a function of (100 keV Si^+) ion dose: (I) for low doses ($< 10^{15}$ cm^{-2}) where amorphization was not complete, crystal growth was observed. (II) For intermediate doses ($(1-5) \times 10^{15}$ cm^{-2}), crystallization through nucleation and growth was found with anomalously high, ion dose dependent nucleation rates, and (III) for sufficiently high doses ($> 5 \times 10^{15}$ cm^{-2}), "normal" nucleation and growth with an ion dose independent nucleation rate was observed. The enhanced nucleation in regime II has been attributed to the presence of c-Si clusters, with typical dimensions smaller than those of stable nuclei, in the surface region of the implanted film.

A piece of the wafer was additionally implanted with 80 keV $^{28}Si^+$ to a total dose of to 5×10^{15} cm^{-2} (i.e. regime III). It may thus be assumed that this sample, which is denoted "spot 6" contains a completely amorphous region at the surface.

Due to the different implantation geometries for the various samples, the position of the deepest a-Si/c-Si interface was not the same for all samples. Channeling measurements show that this depth ranges from 525 nm in sample 1 to 515 nm in sample 6.

3.2. Static reflectivity and Raman spectroscopy

A very simple but effective way to characterize surface structure is a measurement of the optical

reflectivity. As the optical properties of amorphous and crystalline Si are distinctly different [19], the reflectivity is a measure of the crystalline fraction in the amorphous matrix. Using an effective medium calculation, and taking into account the measurement accuracy of 0.1% absolute, the sensitivity limit for detecting c-Si clusters in a shallow a-Si surface region is estimated to be $\approx 2 \times 10^{15}$ atoms/cm^2. The reflectivity, measured using the probe laser, increases from 29.3% for spot 1 to 37.9% for spot 4. This indicates that the crystalline fraction decreases from spot 1 to 4. Reflectivity measurements do not indicate the presence of any crystalline material left in the spots 4, 5 and 6. The sensitivity limit for detecting c-Si in an a-Si surface layer can be improved with about a factor of 5 using Raman spectroscopy [20]. Raman analysis of spots 4, 5 and 6 showed no detectable c-Si, indicating that indeed very few c-Si clusters remain.

3.3. Pulsed laser-irradiation: time-resolved reflectivity

Spots 1 to 6 were irradiated with ruby laser pulses. Fig. 2 shows TRR traces for the 6 spots, all obtained during irradiation at the same energy density of 0.157 ± 0.005 J/cm^2. Clearly, oscillations can be seen in all TRR traces. Such oscillations are characteristic for EC [4–9] and are due to a change in interference condition during propagation of the buried liquid layer. A distinct difference between all transients is observed in the initial reflectivity behavior. Spot 1 shows an initial *increase* in reflectivity, followed by oscillations. This is consistent with the fact that melting is initiated at the buried c-Si/a-Si interface at 60 nm depth. Reflectivity calculations indicate that after formation of a molten layer at 60 nm depth, an interference *maximum* is expected as soon as the liquid layer propagates inwards into the sample.

The transient for spot 2 shows a small initial *decrease* in reflectivity, followed by oscillations. This is in accordance with formation of a buried liquid layer at the c-Si/a-Si interface at 40 nm depth, for which an interference *minimum* is expected.

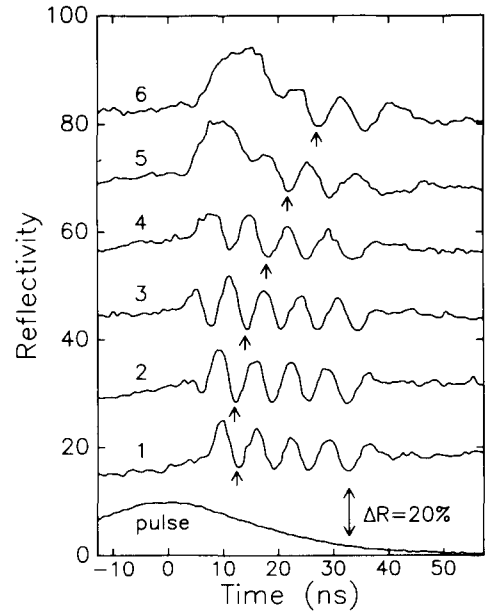

Fig. 2. Transient reflectivity measurements recorded during pulsed-laser irradiation of samples with different surface composition. The numbers 1 to 6 refer to the surface structure (see text). Reflectivity transients are shifted in absolute value for clarity and the reflectivity scale is indicated in the figure. The laser pulse profile is shown at the bottom. Arrows indicate the interference minimum corresponding to 140 nm propagation depth of the liquid layer (see text).

Completely different phenomena are observed for spot 6, with the fully amorphized surface layer. In this case a high-reflectivity phase develops, after which oscillations are observed. This behavior has been observed earlier [4–8] and is explained as follows. During irradiation a primary molten layer forms at the surface, resulting in an increase in reflectivity. c-Si nuclei are formed by one of the nucleation mechanisms as described in section 1 and will grow in this primary melt. After a delay, necessary for growth of nuclei, enough heat is supplied to trigger EC. Hence, oscillations are observed, delayed with respect to the initial increase in reflectivity.

Reflectivity transients for spots 3, 4 and 5 show an intermediate behavior. In all cases an initial increase in reflectivity is observed. These samples do not contain a buried a-Si layer, hence the increase corresponds to melting at the surface. The duration of this surface melt, however, meas-

ured from the width of the first peak, varies from one spot to another. For spot 3, on which a measurement of the static reflectivity before irradiation indicated a small fraction of c-Si clusters, the first peak is only a few nanoseconds wide. For spots 4 and 5 in which the c-Si fraction is expected to be even smaller, the initial peak is broader.

It is interesting to note the difference in timing of the interference oscillations for the various measurements shown in fig. 2. This timing is related to the velocity of the self-propagating buried liquid layer. EC of samples containing a buried amorphous layer proceeds at a relatively constant velocity of ≈ 16 m/s [9,10], whereas EC of an amorphous layer extending to the surface is characterized by a lower velocity [4–8], gradually decreasing to ≈ 11 m/s.

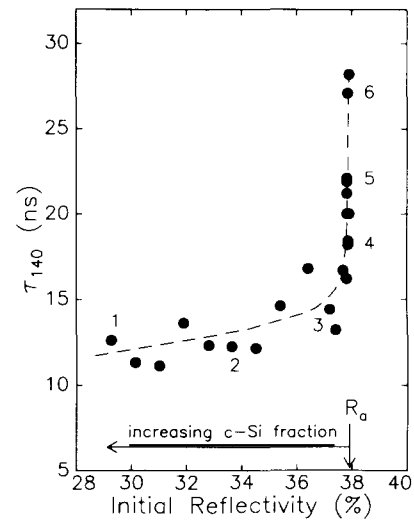

Fig. 3. Timing τ_{140} of the interference minimum corresponding to propagation to a depth of 140 nm (arrows in fig. 2) for different specimens (see text). Timing is taken relative to the peak of the laser pulse. Samples are characterized by the static reflectivity before irradiation. The reflectivity of a-Si (R_a) is also indicated. Numbers in the figure indicate data for spots 1 to 6 as discussed in the text.

4. Discussion

The measurements indicate that the triggering of EC is strongly related to the amount of c-Si material present at the surface. Epitaxial EC is immediately triggered by growth from the c-Si/l-Si interface. Triggering of unseeded EC is delayed and depends on the presence and amount of c-Si clusters at the surface. A qualitative analysis of this effect can be done by measuring the timing of the interference extrema. For this purpose the minimum was used which corresponds to propagation to a depth of 140 nm from the surface.

For spot 1, EC starts at a depth of 60 nm. Optical calculations show that in this case the first minimum (indicated in fig. 2 by an arrow) which can be observed in the TRR transient corresponds to propagation to a depth of 140 nm. For spot 2, EC starts at 40 nm depth, giving rise to a small initial decrease in reflectivity. Propagation to 140 nm depth is then reflected in the second minimum of the TRR transient. For spots 3 to 6, EC starts at the surface, and the second minimum in the transients corresponds to a depth of 140 nm [5,21].

Fig. 3 shows the timing τ_{140} of this minimum for spots 1 to 6, relative to the peak of the laser pulse. Each point represents one measurement of τ_{140}, from the curves shown in fig. 2 as well as from an extended series of TRR measurements. The dashed line serves as a guide to the eye. As the abscissa, the static reflectivity before irradiation is used. The figure shows that for samples with a low initial reflectivity (large crystalline fraction), EC is started relatively early ($\tau_{140} \approx 12$ ns) with respect to the timing of the laser pulse. In samples with a small or no crystalline fraction (high initial reflectivity) EC is started significantly later; τ_{140} increases up to ≈ 28 ns for samples with a fully amorphized surface region. Note that the value of τ_{140} itself has no useful physical meaning, it is the *difference* in τ_{140} which is of concern.

It is emphasized that samples 4 to 6 are almost completely identical; both the thickness of the amorphous layer and the static reflectivity have the same value. Therefore the thermal properties (most important the heat conductivity) are matched. The only difference between samples 4 to 6 is a difference in the density and/or size of crystalline clusters remaining near the surface after the implantation. In all cases this number is too small to be observed directly.

The difference in τ_{140} (i.e. $28 - 12 = 16$ ns) is related to the characteristic time necessary for nucleation and/or growth of c-Si nuclei in undercooled l-Si, in order to trigger EC. It should be noted that the time difference between the actual moment of triggering and τ_{140} depends on the thickness of the c-Si surface layer. A self-propagating buried liquid layer which starts from a deeper lying c-Si/a-Si interface, reaches the depth of 140 nm earlier, resulting in a lower τ_{140}. In order to correct for this effect, the time necessary for the melt front to cover a distance corresponding to the depth of the a-Si/c-Si interface (e.g. 60 nm per 15 m/s = 4 ns) was subtracted from the difference in τ_{140}. A smaller correction is necessary to account for the effect that epitaxial and random EC proceed at a different velocity. This correction amounts to ≈ 1 ns and is also subtracted from the difference in τ_{140}. It can thus be estimated that the characteristic time for nucleation and growth amounts to 11 ± 2 ns. In this context, "growth" is the amount of grain growth necessary to produce sufficient heat for triggering EC.

Similar delay times have been observed by Bruines [6]. He studied the motion of a *freezing* a-Si/l-Si interface and observed growth of c-Si nuclei near the a-Si/l-Si interface. Those nucleation events triggered EC of the a-Si. He found a transient time for triggering of EC, dependent on the freezing velocity: 10 or 20 ns for a freezing velocity of 0.5 or 1 m/s, respectively. Cullis et al. have noted that large concentrations of impurities can suppress the nucleation rate of c-Si in undercooled l-Si [22]. In the present experiments the copper concentration in the region where EC is triggered is less than 2 ppm. Although an influence on the nucleation rate cannot be strictly excluded, we expect this concentration to be too low for such an influence.

5. Conclusions

A range of sample structures consisting of an amorphous Si layer on top of a crystalline Si substrate has been prepared by ion implantation. The thickness of the a-Si layer is essentially the same for all samples, but the condition of the outer surface varies from a thin layer of single crystal Si covering the a-Si layer to a completely amorphized surface containing a variable number of small crystalline clusters. Explosive crystallization (EC) in these samples is triggered by low-energy pulsed-laser irradiation. When the a-Si layer is covered by a thin layer of single crystal Si, EC is immediately triggered by epitaxial growth from the c-Si surface layer, with no delay. In the absence of a seed for crystallization, EC is triggered by nucleation and growth of crystallites in a thin molten layer at the surface and is delayed by 11 ± 2 ns in comparison to the previous case. The delay time measured on samples containing c-Si clusters varies between 0 and 11 ns, depending on the density of clusters. The two types of EC are found to proceed with a different velocity. Epitaxial EC travels at a constant speed of ≈ 16 m/s whereas unseeded EC proceeds somewhat slower at a velocity decreasing to ≈ 11 m/s.

Acknowledgements

It is a pleasure to acknowledge F.W. Saris for critically reading the manuscript and for stimulating discussions and A.J.M. Berntsen (RUU) for assistance with Raman spectroscopy. This work is part of the research program of FOM and was financially supported by the Nederlandse Organisatie voor Wetenschappelijk Onderzoek (NWO) and the Stichting Technische Wetenschappen (STW).

References

[1] M.O. Thompson, G.J. Galvin, J.W. Mayer, P.S. Peercy, J.M. Poate, D.C. Jacobson, A.G. Cullis and N.G. Chew, Phys. Rev. Letters 52 (1984) 2360.
[2] W.C. Sinke and F.W. Saris, Phys. Rev. Letters 53 (1984) 2121.
[3] J. Narayan, S.J. Pennycook, D. Fathy and O.W. Holland, J. Vacuum Sci. Technol. A2 (1984) 1495.
[4] D.H. Lowndes, G.E. Jellison, S.J. Pennycook, S.P. Withrow and D.N. Mashburn, Appl. Phys. Letters 48 (1986) 1389.
[5] J.J.P. Bruines, R.P.M. van Hal, H.M.J. Boots, A. Polman and F.W. Saris, Appl. Phys. Letters 49 (1986) 1160.
[6] J.J.P. Bruines, Time-resolved study of solidification phe-

nomena on pulsed-laser annealing of amorphous silicon, Thesis, Eindhoven Technical University (1988).
[7] D.H. Lowndes, S.J. Pennycook, G.E. Jellison, S.P. Withrow and D.N. Mashburn, J. Mater. Res. 2 (1987) 648.
[8] D.H. Lowndes, S.J. Pennycook, R.F. Wood, G.E. Jellison and S.P. Withrow, Mater. Res. Soc. Symp. Proc. 100 (1989) 489.
[9] A. Polman, D.J.W. Mous, P.A. Stolk, W.C. Sinke, C.W.T. Bulle-Lieuwma and D.E.W. Vandenhoudt, Appl. Phys. Letters 55 (1989) 1097;
P.A. Stolk, A. Polman, W.C. Sinke, C.W.T. Bulle-Lieuwma and D.E.W. Vandenhoudt, Mater. Res. Soc. Symp. Proc. 147 (1989) 179.
[10] A. Polman, P.A. Stolk, D.J.W. Mous, W.C. Sinke, C.W.T. Bulle-Lieuwma and D.E.W. Vandenhoudt, J. Appl. Phys. 67 (1990) 4024.
[11] E.P. Donovan, F. Spaepen, D. Turnbull, J.M. Poate and D.C. Jacobson, Appl. Phys. Letters 42 (1983) 698.
[12] J.Y. Tsao and P.S. Peercy, Phys. Rev. Letters 58 (1987) 2782.
[13] S. Roorda and W.C. Sinke, Appl. Surface Sci. 36 (1989) 188.
[14] S.R. Stiffler, M.O. Thompson and P.S. Peercy, Phys. Rev. Letters 60 (1988) 2519.
[15] This, and other related topics concerning nucleation, are discussed in detail in: W.C. Sinke, A. Polman, S. Roorda and P.A. Stolk, Appl. Surface Sci. 43 (1989) 128.
[16] D.H. Auston, C.M. Surko, T.N.C. Venkatesan, R.E. Slusher and J.A. Golovchenko, Appl. Phys. Letters 33 (1978) 437.
[17] W.K. Chu, J.W. Mayer and M.A. Nicolet, Backscattering Spectrometry (Academic Press, New York, 1978);
L.R. Doolittle, Nucl. Instr. Methods B9 (1985) 344.
[18] R.B. Iverson and R. Reif, Appl. Phys. Letters 52 (1988) 645.
[19] R.F. Wood and G.E. Jellison, in: Semiconductors and Semimetals, Vol. 23 (Academic Press, New York, 1984).
[20] E. Bustarret, M.A. Hachicha and M. Brunel, Appl. Phys. Letters 52 (1988) 1675.
[21] A more elaborate analysis is necessary for the TRR transients for spots 5 and 6. In these transients a long high-reflectivity phase is observed which could shield interference extrema. In that case, the minima indicated by arrows in fig. 2 could correspond to propagation to a depth of 240 nm rather than 140 nm. This problem has been studied extensively in earlier work using pulsed-laser irradiation of a-Si surface layers [5]. In those experiments it was found that just above the melt threshold (as in the present experiments) the second minimum in the TRR traces indeed corresponds to propagation to a depth of 140 nm.
[22] A.G. Cullis, N.G. Chew, H.C. Webber and D.J. Smith, J. Crystal Growth 68 (1984) 624.